

CHAPTER 1

INTRODUCTION AND LITERATURE REVIEW

- 1.1 Introduction**
- 1.2 Overview of different HPM devices**
 - 1.2.1 Relativistic Backward Wave Oscillator**
 - 1.2.2 Relativistic Klystron**
 - 1.2.3 Relativistic Magnetron**
 - 1.2.4 Relativistic Gyrotron Devices**
 - 1.2.5 Reltron**
 - 1.2.6 Virtual Cathode Oscillator**
- 1.3 Magnetically Insulated Line Oscillator (MILO)**
 - 1.3.1 Description of sub-assemblies**
 - 1.3.2 Principle of Operation**
- 1.4 Literature Review**
- 1.5 Motivation and Research Objective**
- 1.6 Plan and Scope**

1.1. Introduction

Over the past few decades, high-power microwave (HPM) has been very popular in the microwave community due to its various civilian and military applications and the technological advancement all around for the device developments. The generation of RF in millimetre-wave ranges and dual-frequency generation through a single HPM device drag the attention of researchers and academia around the world for R&D in this domain. HPM, by convention, includes both the microwave and millimetre-wave frequency ranges (1-100 GHz) producing peak power $>100\text{MW}$ and refer to (i) the long pulse duration, high-pulse repetition frequency (PRF), or continuous wave (CW) or (ii) the high-peak-power, short-pulse duration, low-PRF, or single-shot sources and amplifiers. The domain of application of HPM devices at a different frequency and Power level is given in Fig. 1.1.

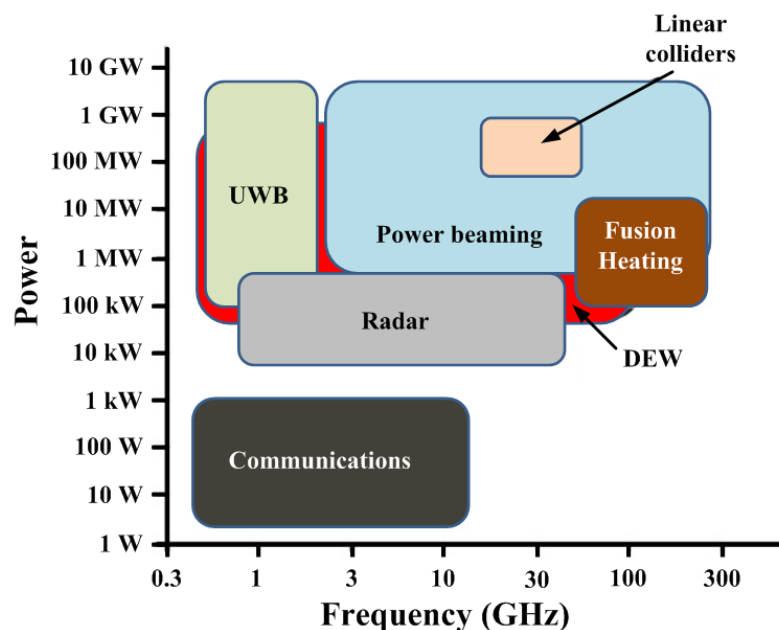


Figure 1.1: Application domain of HPM at a different frequency and Power level [Benford *et al.* (2007)].

Table 1.1: Application of HPM device in different domains [Benford *et al.* (2007)].

Industrial	Industrial plasmas, especially for semiconductor manufacture Testing and Instrumentation Materials processing
Scientific	Ground Penetrating Radar Medical/Biomedical Atmospheric radar Charged particle accelerators Spectroscopy Materials Processing Research Radio astronomy Plasma heating and fusion energy research Deep space communications
Civilian Infrastructure and consumer markets	Global Positioning System (GPS) Satellite communications Radar, e.g.: Air traffic control, Weather, Maritime Broadcast media transmission (TV, radio), Cellular (wireless) communications
Military	High Power Microwave (HPM) Electronic Attack Radar: Guidance, Search, Missile-seeker, Track, Weather, Test Electronic Counter Measures(ECM)

HPM has both civilian and military applications which are briefly summarized in table 1.1. The HPM devices can be categorized based on the existing or potential applications of these sources, like (a) high-average power oscillators in resonance heating and current drive of thermonuclear fusion plasmas; (b) microwave and millimetre-wave narrow band sources and amplifiers for RF acceleration in high-energy linear colliders; (c) broadband millimetre-wave amplifiers in radar and communication

systems and (d) high-peak-power sources for direct energy weaponry (DEW) of both the hard-kill type, which aims at the physical destruction of targets and the soft-kill type, which makes the enemy's mission-critical components either inoperative or faulty. To achieve this, the peak output power of the RF signal must be in the range of a few GW, and the pulse width of the signal must be nearly equal to 100 ns in microwave and millimetre-wave frequency ranges.

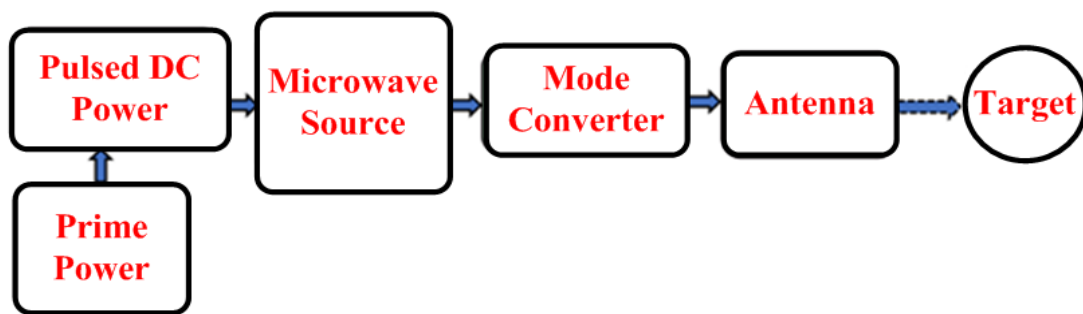


Figure 1.2: Block diagram of an HPM system [Benford *et al.* (2007)].

The block diagram describing the HPM system is shown in Fig. 1.2. The different subsystems of the whole HPM system have a unique role in the whole process of RF generation and application.

- (i). **Prime Power:** Prime power supply produces a relatively low power electrical signal in a long pulse or continuous mode. For linking the prime power to the pulse power supply, the crucial parameters are the average power, the repetition rate that simultaneously defines the energy per pulse, and the output voltage. The prime power supply comprises of four main components i.e. internal combustion as a prime power producing an AC output; an interface component like a pump, motor, controller or AC to DC converter; followed by energy storage and

electrical source component; connected with AC or DC converter. The output of prime power provides a series of switched DC pulses to the pulsed power source.

- (ii). **Pulsed Power:** In general, HPM sources needs drivers that can supply short, intense electrical pulses of 1 MV or more for upto 1 μ s duration. This can be achieved by using either pulse compression or use of capacitor banks that can convert low-voltage, slowly increasing signal into high-voltage, fast-rising signal.
- (iii). **HPM Source:** The HPM source which is the main building block of the whole HPM system follows three basic operations which are the generation of the electron beam, efficient beam-wave interaction, and extraction of the generated RF signal. The elementary procedure behind all vacuum electron beam sources is the resonant interactions that occurred between the natural oscillation modes of the electron plasma and the eigenmode of cavities and/or waveguides.
- (iv). **Mode Converter:** To achieve the highest impact on the target, the radiated EM wave must be of proper mode. Some of the HPM sources generate azimuthally symmetrical modes having null in the direction of propagation. Such azimuthally symmetrical modes are converted to required modes having maximum power in the direction of propagation by using a suitable mode converter. Thus, the mode converter is used for tailoring the spatial distribution of electromagnetic energy to optimize the transmission of RF power and coupling to an antenna.
- (v). **Antenna:** The microwave radiator, like an antenna, acts as the interface between the HPM source and the rest of the space. The RF energy coming out from the mode converter is further radiated towards the target through the antenna which

compresses the output spatially into a tighter and high-intensity beam. The rectangular horn antennas are the most common type of antennas used in HPM sources.

1.2. Overview of different HPM Sources

High power microwave (HPM) sources are generally classified in two different ways: one is on the basis of its frequency band generation which is ultra-wideband electromagnetic radiation and narrowband HPM sources and another on the basis of beam-wave interaction mechanism [Gold and Nusinovich (1997), Smith and Cloude (2002)].

Narrowband HPM sources generate coherent radiation with the expense of mono-energetic electron beam's kinetic energy in pulses ranges from 10's-100's ns in duration. Whereas, ultra-wideband sources use no electron beam, but, uses a high voltage spike with a very short rise time. The antenna radiates this high voltage spike through coupling in the wide frequency range. Ultra-wideband is considered analogous to flashbulbs.

There is basically three kinds of electromagnetic (EM) radiation which any HPM sources support on the basis of interaction mechanism between the relativistic electron beam and RF structure:

- (i). **Cherenkov Radiation:** HPM sources in which electrons propagate in a medium having the refractive index $n > 1$ and the electron velocity v_e exceeds the phase velocity $v_{ph} = c/n$ of EM waves supports Cherenkov radiation. When the refractive index is so large (i.e. $n > c/v$) then only the interaction can produce

this radiation. The different HPM sources which are based on Cherenkov radiation are Travelling wave tube (TWT), Relativistic backward wave oscillator (RBWO), Relativistic magnetron, and MILO. Cherenkov HPM sources can produce several GW of RF output power in 1-10 GHz frequency range for a very short period of time (i.e. 10-100 ns) and also operates at a repetition rate of several 100 Hz.

(ii). **Transition Radiation:** The HPM sources in which transition radiation occurs are having some conducting grids or plates for perturbation of electron beam. Whenever electrons pass through a border between two media having different refractive indices, transition radiation occurs. The different HPM sources which produce transition radiation are the relativistic klystron oscillator (RKO), relativistic klystron amplifier (RKA), and the Reltron [Barker and Schamiloglu (2001)]. These devices can produce RF output power up to 10's of GW in pulse duration of 100 ns at frequencies in 1 GHz.

(iii). **Bremsstrahlung Radiation:** HPM sources in which electrons oscillation occurs in external magnetic and/or electric field, generates Bremsstrahlung radiation. When Doppler-shifted frequencies coincide with either electron frequency oscillation Ω or with its harmonics through $\omega - k_z v_z = s\Omega$, electrons radiate EM waves. Here, $k_z v_z$ is the Doppler-shift and s is the resonant harmonic number. The radiated wave can be fast or slow as the expression satisfies for all wave phase velocity. The HPM sources which are based on bremsstrahlung radiation are Cyclotron resonance masers (CRM) and Free Electron Laser (FEL). Bremsstrahlung radiation-based sources can produce EM radiation across a very broad frequency range that extends well above 100 GHz and are tunable in nature. Vircators or

virtual cathode oscillators are considered as the special type of Bremsstrahlung device in which electrons oscillate in an external electromagnetic field [Gold and Nusinovich (1997)]. This device can be treated as an extreme case of the intense beam relativistic klystron amplifiers (RKAs) in which space-charge causes voltage depression which significantly enhances the electron velocity modulation and bunching.

1.2.1. Relativistic Backward Wave Oscillator (RBWO)

A relativistic backward-wave oscillator (RBWO) is an HPM device that uses an intense relativistic electron beam to generate an EM wave with negative group velocity where the wave is traveling in the direction opposite to the electron beam. Fig. 1.3 shows the typical schematic view of RBWO. It consists of an intense electron beam forming cathode, external magnetic field, collector, and cylindrical metallic structure with axial periodicity formed by a sinusoidal ripple on the wall. An intense relativistic electron beam propagates axially under the influence of a strong external magnetic field which excites the EM mode supported by the slow-wave structure (SWS) and generates the EM wave with the expense of kinetic energy of the electron beam. To extract out the EM wave axially from the device, a cavity resonator or cut-off waveguide section is widely used to reflect the TM_{01} mode (i.e. the fundamental mode of operation) backward wave to a TM_{01} mode forward wave.

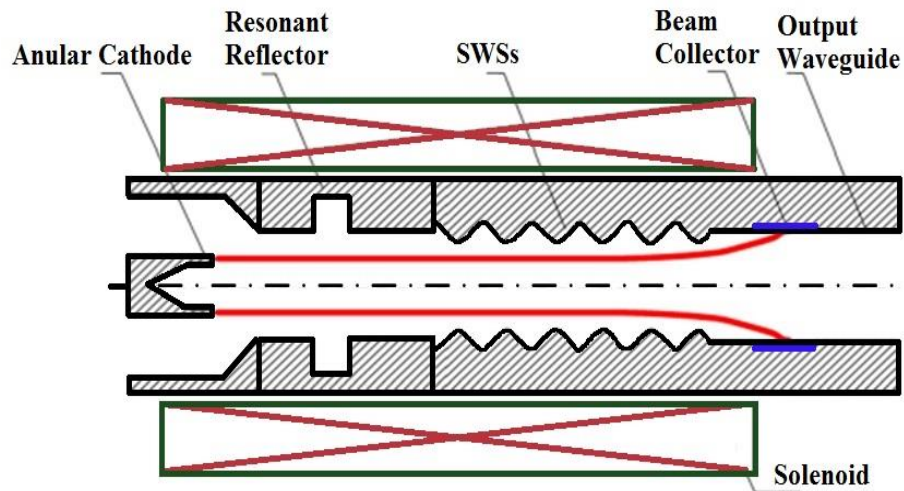


Figure 1.3: The typical schematic view of relativistic backward wave oscillator.

1.2.2. Relativistic Klystron

The relativistic klystron is a popular HPM source that is widely used in charge particle physics and RF linear accelerator (Linacs) applications. The typical schematic view of the relativistic klystron is shown in Fig. 1.4. It consists of a cathode that generates an electron beam of the desired parameter, two or more pillbox cavities separated by a drift tube, extraction waveguide, and RF output window. As the electron beam enters between grids of the buncher cavity, some of the electrons group accelerates while others get decelerated; thereby forming electrons bunches with different velocities. At the catcher cavity of the device, the electron bunch releases their kinetic energy to the RF waves. Finally, the unused electrons are collected at the collector subassembly of the klystron. The operation of relativistic klystron is similar to that of the conventional klystron. In the relativistic klystron, the high energy electrons and the relativistic effects change the modulation process as compared to the conventional klystron. These high-energy electrons in the form of thin annular electron beam propagate near the outer wall

of the structure and carry much higher current at a given DC voltage [Barker *et al.* 2001]. The relativistic klystrons are widely used as high energy drivers for free-electron lasers, directed energy weapons, colliders, and accelerators [Benford *et al.* (2007)].

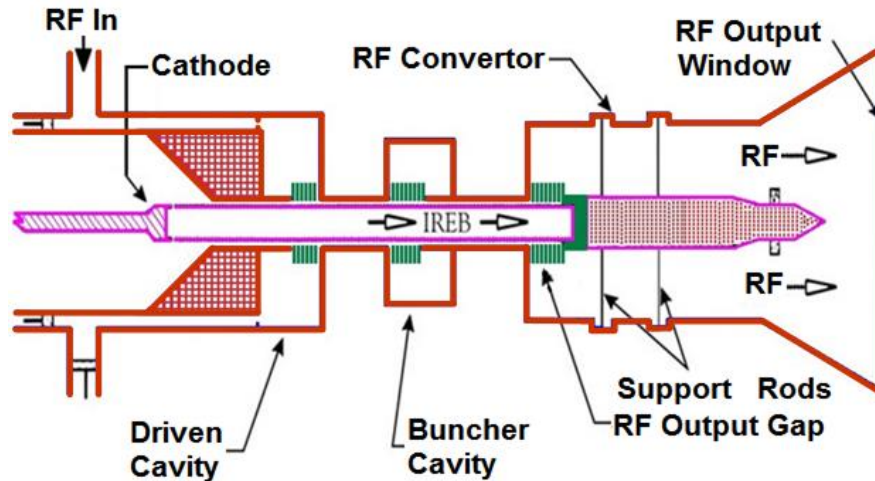


Figure 1.4: The typical schematic view of relativistic Klystron [Gold and Nusinovich (1997)].

1.2.3. Relativistic Magnetron

The relativistic magnetron originates due to the development of cold cathode and pulsed power technology. It is a high voltage, high current version of the well-known conventional magnetron. The conventional magnetrons had reached power up to 10 MW whereas the first relativistic magnetron produced 900 MW power [Benford *et al.* (1987), Benford (2010)]. This source was developed as a direct extrapolation of the cavity magnetron, driven at high currents which are produced by pulsed-power, and cold-cathode technology. The relativistic magnetron is the high-current extension of conventional magnetrons, where the ‘relativistic’ voltage is required to produce the high currents [Benford *et al.* (1987)]. The relativistic magnetron operates in the frequency

range of 1-10 GHz. The typical schematic view of relativistic magnetrons is shown in Fig. 1.5. The cathode is surrounded by the anode cavity structure as seen in Fig. 1.5. The area between the cathode and anode is called the interaction region, or the A-K gap, where the conversion of input electrical power to RF power takes place. A negative voltage is applied to the cathode and the anode block is held at ground potential, an axially oriented magnetic field is applied additionally. From the mathematical relations known as the Buneman-Hartree condition and the Hull cut-off condition, approximate operating voltages and magnetic fields can be calculated. When these values are applied to a properly designed magnetron, electrons are emitted from the cathode, and their energy is converted to microwave energy which is extracted out utilizing a loop through one of the cavity.

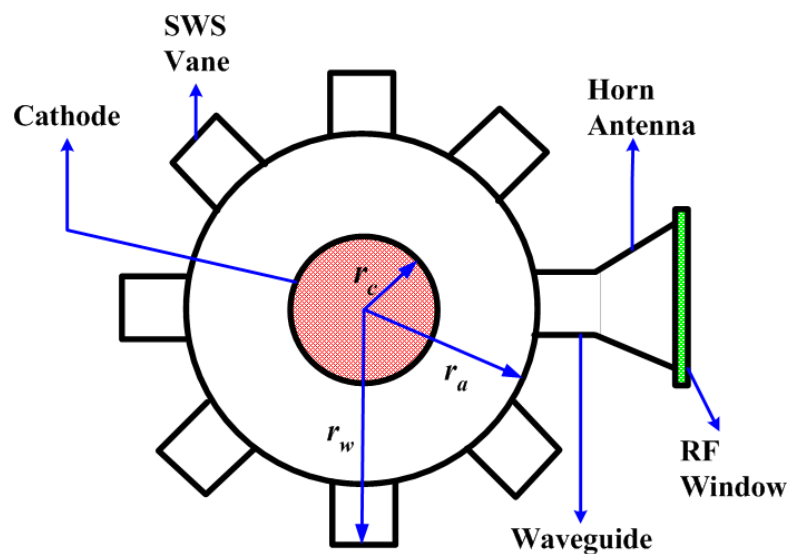


Figure 1.5: The typical schematic view of relativistic Magnetron [Bekefi *et al.* (1976)].

1.2.4. Relativistic Gyrotron Devices

Gyrotron is also known as the ‘electron cyclotron resonance maser’ and it is a high power high-frequency source. In gyro-devices, the phase velocity of the EM wave in the

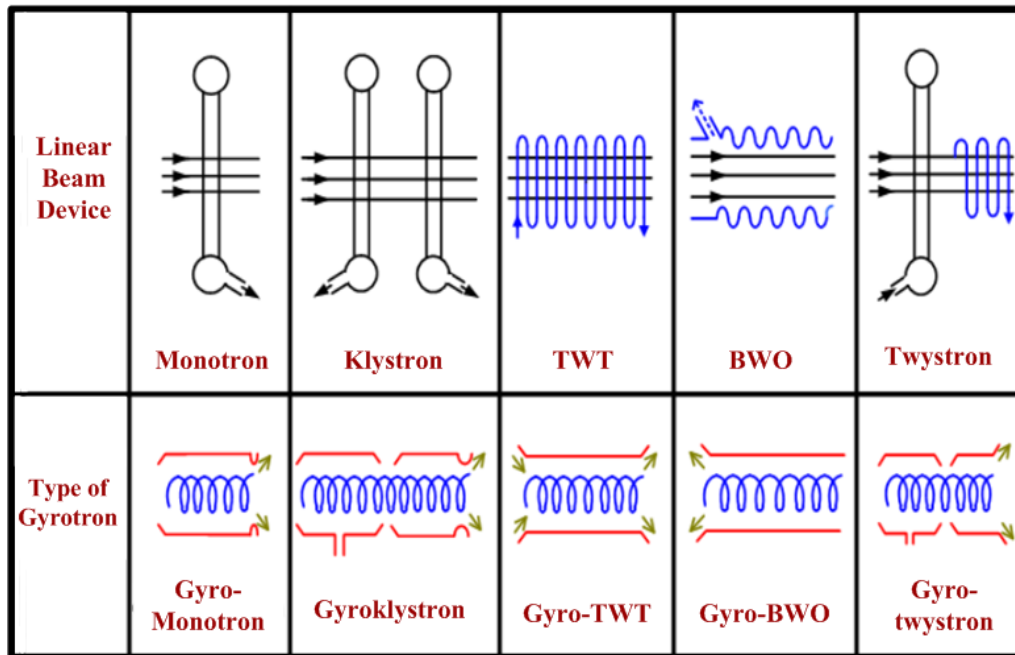


Figure 1.6: All types of Gyro-devices [Gold and Nusinovich (1982)].

interaction circuit is greater than or equal to the speed of light. Gyrotron comprises of magnetron injection gun, which produces an annular gyrating electron beam that is guided in an open cavity resonator by a high external axial DC magnetic field produced by a superconducting magnet. The magnitude of the applied DC magnetic field and the microwave frequency that can be generated from the device are closely related to the synchronism condition. The beam wave interaction inside the cavity uses the cyclotron motion of the electrons present in the beam and the transverse kinetic energy of the electrons is converted into the RF wave resulting in the formation of a Gaussian wave. The spent electrons, after losing their energy, flow out of the beam cavity and propagate to the collector where it is finally collected. The particular variation of the gyro-device based on the interaction circuit falls into several categories as per their conventional device counterparts, like, gyrotron oscillator also known as gyro-monotron, gyro-TWT,

Gyro-klystron, gyro-BWO, gyro-twystron, etc. Fig. 1.6 shows different types of gyrotron devices for their slow-wave and fast-wave.

1.2.5. Reltron

The Reltron is relatively new in HPM source which is capable of producing several hundreds of MW power in the frequency range of 1-12 GHz. [Mahto and Jain (2016)]. Fig. 1.7. shows the schematic view of the reltron oscillator. The reltron system comprises of high voltage pulser as input power supply, voltage divider circuit, explosive cathode, Side-coupled cavity as RF interaction cavity or modulating cavity, post-acceleration mechanism, extraction cavity, and finally a beam dump. A high DC pulsed voltage from the power supply is divided into two parts with the help of a voltage divider circuit. One part of the power supply is provided to the explosive cathode to generate very high-density electrons beam and the other part are used at post-acceleration region to re-accelerate the electron bunches emerging from RF interaction cavity. The electron bunching mechanism i.e. density modulation is just similar to the klystron source with some differences that is it modulates the electrons beam twice in the modulating cavity and then re-accelerate the bunches using post acceleration mechanism and finally it does not require any external DC magnetic field to guide the electron beam [Benford *et al.* (2006)]. The device operates primarily in TM_{01} mode, but the generated RF is extracted out in TE_{10} mode using a rectangular waveguide therefore the device does not require any external mode converter. For long pulse operation up to a few microseconds or for large energy per pulse operation another variant of reltron was reported that was based on thermionic emission cathode [Benford *et al.* (2007)].

The Reltron was firstly developed in the year 1992 by Titan Advanced Innovative Technologies of Albuquerque, NM, USA. The major advantages of reltron are that it can produce microwave pulse widths approaching $1 \mu\text{s}$ and pulse energies of a few 100 joules, outstripping the other HPM devices, like, relativistic magnetrons that are limited to pulse widths of about 100 ns and pulse energies below 100 J. Apart from these, frequency tunable reltron can be tuned $\pm 10\%$ with respect to central frequency [Gold and Nusinovich (1997)].

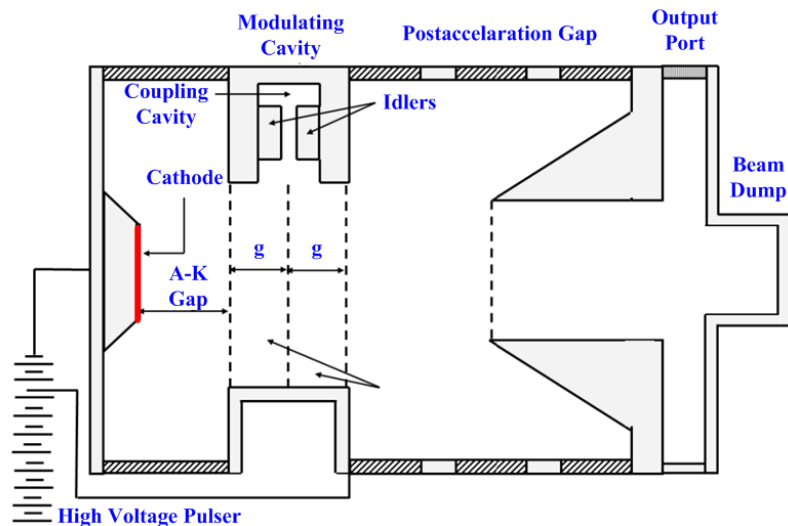


Figure 1.7: Typical schematic of reltron oscillator system [Mahto and Jain (2016)].

1.2.6. Virtual Cathode Oscillator

Virtual cathode oscillator or vircator is differing from the rest of the HPM sources in the way of generation of RF signal. Unlike the other HPM sources, the vircator has no conventional counterparts. It can operate in a very large frequency range varying from 300 MHz to 40 GHz without an external magnetic field. It is very compact and lightweight with a feature of frequency tunability. Vircator has the main drawback that it has very low efficiency comparing with the other HPM sources. The typical

schematic view of the virtual cathode oscillator is shown in Fig. 1.8. It consists of a high voltage pulser, cathode, anode foil, and RF window. The physics behind this device is the formation of a virtual cathode. The formation of a virtual cathode in the device takes place when the current associated with the electron beam exceeds the space charge limiting current derived by Child-Langmuir. To achieve this, generally the structure in which the electron beam propagates having a metallic tube with different radii. Due to the sudden change in radius, the beam slows down and some electrons reverse their direction, creating a high space-charge density region and an electrostatic potential depression takes place which is known as a virtual cathode. After the virtual cathode formation, some of the electrons having sufficient kinetic energy cross the virtual cathode while the remaining electrons oscillate in between the physical cathode and the virtual cathode, and this leads to the growth of the electromagnetic waves in the virtual cathode oscillator. The operating mode of virtual cathode oscillator is TM mode and therefore, mode conversion becomes a necessary part for RF extraction [Benford *et al.* (2007), Granatstein and Alexeff (1987)]. To improve the performance of the vircator, the multistage axial vircator has been developed [Champeaux *et al.* (2015)].

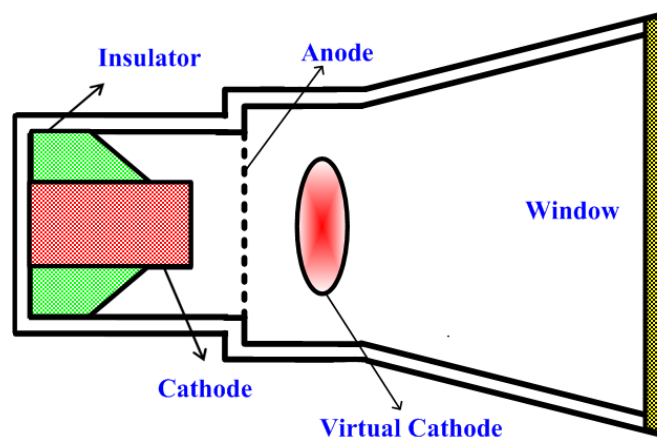


Figure 1.8: The typical schematic view of the virtual cathode oscillator.

Table 1.2: Comparison of MILO with other HPM Sources.

Parameters	MILO	Viricator	Reltron	Relativistic Magnetron	Relativistic BWO	Relativistic Klystron
Operating Frequency	Up to <i>Ku</i> -band	Up to <i>X</i> -band	Up to <i>X</i> -band	Up to <i>X</i> -band	Up to <i>Ku</i> -band	Up to <i>Ku</i> -band
Efficiency	20-30 %	1 – 3 %	30-40 %	20-30 %	40 %	35-60 %
External Magnetic field Requirement ?	No	No	No in gridded; Yes in gridless	Yes	Yes	Yes
Size	Compact	Compact	Heavy	Heavy	Heavy	Heavy
Impedance	Low	Low	High	High	High	High
Osc. or Amp.	Osc.	Osc.	Osc.	Osc.	Osc.	Osc./Amp
Construction complexity	Easy	Easy	Complex	Complex	Easy	Easy
Oscillation mode	TM ₀₁	TM _{0n}	TE ₁₀	TM ₀₁	TM ₀₁	TM ₀₁
Frequency tuning with Input voltage	No	No	No	Yes	Yes	No
Repetitive	Up to 20 Hz	Single shot	Single shot	Up to 250Hz	Up to 100 Hz	No

1.3. Magnetically Insulated Line Oscillator (MILO)

The magnetically insulated line oscillator (MILO) is a crossed-field high power microwave device that is similar in operation and theory of magnetron thus also known as a linear magnetron. It operates combining the technology of magnetically insulated

electron flow and slow-wave tubes. Microwave oscillators that require an external magnetic field employ two DC power sources to exhibit magnetic insulation and also lead to electrical breakdown when exposed to high voltages. These oscillators are having a very high inherent impedance that severely limits the power level at which the oscillator will operate. Thus, for efficient operation at higher power levels, it would be desirable to have an oscillator that will operate at the lower impedance and also eliminate the problem of voltage matching [Bekefi *et al.* (2006)]. To overcome the above problems, MILO has been used, in which the required magnetic field is supplied by the electron-beam current itself, rather than by a separate magnet and thus makes the device more compact and lightweight. The comparison of MILO with other HPM sources is given in table 1.2 which shows the importance of this device comparing with other HPM sources.

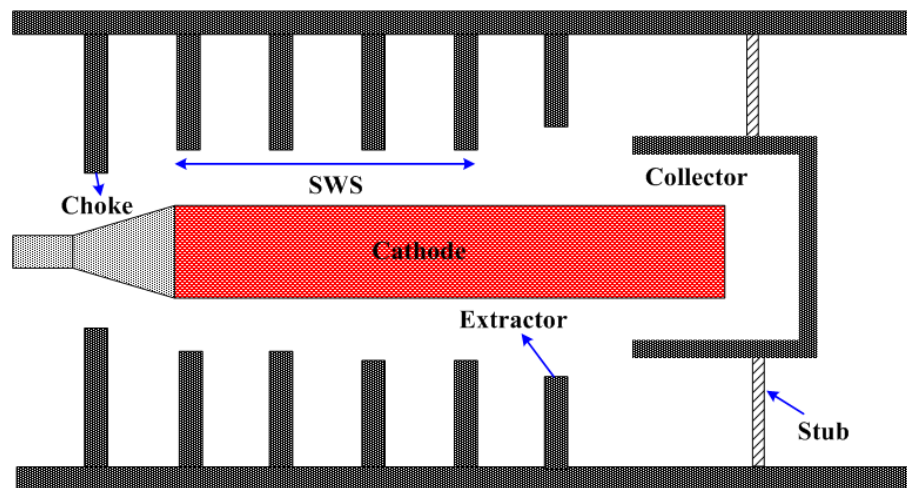


Figure 1.9: The typical schematic view of a magnetically insulated line oscillator (MILO).

1.3.1. Description of sub-assemblies

The typical schematic view of the conventional MILO device is shown in Fig. 1.9. It consists of a periodic disc loaded coaxial structure which work as a slow-wave structure (SWS), the inner conductor used as explosive emission cathode, first few discs towards input side act as a filter or chokes cavity, one cavity toward output side act as extractor cavity, inductive stub used to provide feedback path, and collector to collect electrons.

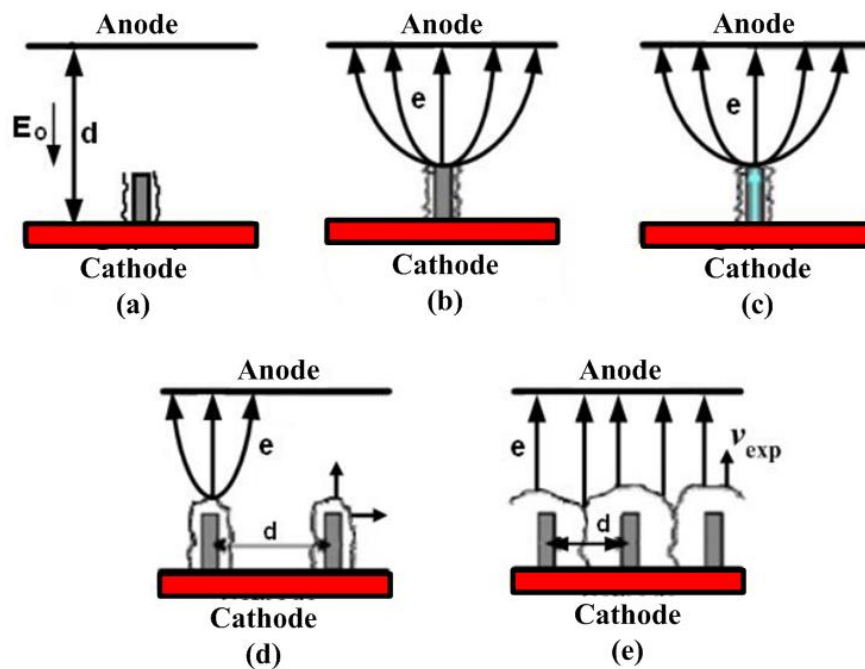


Figure 1.10: Process of electron emission from a velvet surface: (a) The application of the intense electric field causes the partial destruction of fiber and the creation of a dense plasma column. (b) Electrons are emitted out of plasma and form a space charge current of the Child-Langmuir type. (c) Heating occurs in fiber due to the Joules effect. (d) Expansion of the plasma column at the thermal speed, and (e) Reduction of inter-electrode space by the total expansion of the plasma of the cathode [Miller (1998)].

(i). **Cathode:** The cathode used in the MILO device is an important sub-assembly that provides a suitable electron beam for the operation of the device. MILO is a gigawatt class device that requires explosive emission cathode because such cathodes “turn-on” at relatively low electric fields and deliver the very high-current densities of 100’s of A/cm² that allow the tube to generate extremely high RF power. Cathode surface of the device is conventionally covered with the velvet for explosive electron emission (EEE) because it is inexpensive and has a low electric field threshold (<30kV/cm) for plasma initiation, it can emit a very high current density (>1kA/cm) and have a low plasma closure velocity [Adler *et al.* (1985), Miller (1998)]. The cold cathodes subjected to an intense electric field satisfy the law of the field emission. When electrons acquire sufficient potential energy that is either by a rise in temperature or due to the application of an intense electric field, they tear off. In MILO, for the electron emission, the explosive emissive cathode is used. In such type of cathode a very high electric field is applied at the surface of the cathode (with the application of very high voltage between anode and cathode) which results the emission of electron with high kinetic energy (i.e. electrons leaving the cathode surface very quickly). The quick departure of electrons from cathode surface is termed here as ‘tear off’ or “tearing off electrons”. This is accelerated by the potential difference between the cathode and the anode. Fig. 1.10 shows the emission process of the velvet cathode.

There are so many different types of cathode that are used in place of velvet cathode. Dielectric fiber has been used as the cathode which initiates surface flashover mechanism when the electric field exceeds 20 kV/cm [Miller (1998)]. Carbon fiber cathodes impregnated with cesium iodide (CsI) salt have proven to be

a better choice than standard velvet cathodes. It has advantages including lightweight and requires no heater for electron emission. In order to improve the pulse repetition rate and the maintenance-free lifetime of MILO, a metal-dielectric cathode can be used [Fan *et al.* (2008)]. More recently, MILO devices have used metal array cathodes (MAC), which have a much longer lifespan and a much lower recurring rate than velvet and bring a promising approach to the repetitive operation of MILO [Qin *et al.* (2016)].

(ii). **Choke cavity:** MILO device uses periodic disc loaded coaxial structure in which the first few discs forming choke cavity. The choke cavity mainly acts as a low pass filter which stops the leakage of RF toward the input DC source. It also acts as the in-phase reflector enhancing the beam-wave interaction and reducing the load on the DC pulse power source. In addition, the impedance difference between the last choke disc and the first primary disc causes the electron flow in the primary SWS to move closer to the cavity openings where the RF voltage is strongest. This increases power conversion efficiency. At lower impedance, there is more current in the electron flow, and therefore, more power available for microwave generation. The first experimental prototypes developed at Kirtland by the US Air-Force did not have this choke [Lemke and Collin (1987)]. The Sandia team proposed to consider an anode structure or the first discs stack have openings smaller than those that occurs at the interaction and the energy exchanges in the structure.

(iii). **RF interaction structure or Slow-wave structure (SWS) cavity:** MILO consists of a number of metal coaxial discs as the slow-wave RF interaction structure. One period of disc forms a cavity. The interaction cavities oscillate in their fundamental

TM mode. At this mode, each cavity behaves as a quarter-wave oscillator shifted in phase by π from its adjacent cavity. Thus, the RF interaction cavity oscillates at π mode, which is not a propagating mode and makes it possible to store large electromagnetic energy.

(iv). **Extractor cavity:** Extraction cavity design is also an important factor to affects MILO output power. In order to achieve maximum power output, the inner radius of the last SWS disc called the extractor disc is made and increase to match the electric field near SWS of the device to the electric field at the coaxial transmission line and achieve the best match for maximum output of microwave extraction. In MILO, power is extracted axially and for efficient power extraction, it is important to couple the oscillation cavity with the guide of exit. Here extractor provides such coupling and fixes the opening by which power is extracted and propagated towards the outside. The axial distance from the extractor disc and the coaxial transmission line is called the extractor gap. The inner radius of the extractor disc is slightly larger than the rest of the discs to provide a good match of the extractor gap electric field to that of the output coaxial transmission line (CTL). Extractor converts standing wave into a traveling wave which is to propagate outside.

(v). **Collector:** The main function of the collector is to collect the unspent electrons after beam-wave interaction. The collector is also acts as load with a portion of the cathode surface area which is covered inside the collector. Hence, the MILO collector does not merely collect the unspent beam but its dimension fixes the geometry of the beam, conditions of magnetic insulation as well as the oscillation conditions. The main object of deciding the collector length is to also show the influence of the length of coverage on the coupling of the output resonator cavity.

The covering of the collector on the cathode constitutes an additional cavity that couples the RF interaction SWS which includes the periodic resonators, cavity under the collector, and the exit waveguide [Cousin (2005)].

(vi). **Stub:** Stub rod at the output side of the MILO device is mainly used to provide a feedback path for current so that the magnetic insulation can take place in the device. It is inductive in nature and works as DC short and RF open. It also provides impedance matching at the output for maximum power conversion efficiency.

1.3.2. Principle of Operation

The MILO operation is divided into four basic stages which start with the emission of electrons from the cathode surface, and then magnetic insulation condition attained by the device followed by noise formation and beam-wave interaction and finally ends with the extraction of RF energy out of the device.

Electron emission: The UHF (ultra high frequency) pulse device, driven by high-potential is applied between cathode-anode structures. This device is responsible for the distributed electron emission from the cathode surface and accelerated by the potential difference between cathode and anode.

Magnetic insulation: The minimum current needed to generate the self-magnetic field to create the insulation between the anode and cathode is called critical current. When the anode current is more than the critical current, all the electrons are confined between the anode and cathode due to the self-magnetic field generated by the anode current. This is the basic concept for producing very high-power microwave pulses in a device

called MILO. Conditions of magnetic cut-off and interaction in the device are controlled by the load current. Further, the load current is decided by the space between the collector and cathode.

Noise formation and Beam-wave interaction: Because of fluctuations in the emission process and noise-amplifying effects in the space-charge Hub (Beam current) between cathode-anode, electron velocities and the charge density in the flowing space-charge cloud fluctuate randomly with time and produce a noise component to the beam current in the space charge hub. The frequency of the fluctuations varies over such a wide range that the noise is referred to as “white noise,” which implies fluctuations over an infinite frequency range. While the frequency range of fluctuations is not infinite, it is rich in components in the microwave range, and so there are components present to initiate any of the frequencies that may be supported by the SWS cavity of MILO. This noise current in the hub induces noise current in the cavities. When the component of this noise current that is at the resonant frequency of the cavities passes through a high impedance of the cavities at one of the resonant frequencies, RF voltages are produced across the cavity gaps and these amplify the RF current in the hub. RF current and power build-up rapidly and saturate when the power supplied to the MILO equals the power to the load plus losses.

When the synchronism condition is arranged such that the axial velocity of the electron flow is equal to the phase velocity of the RF waves in the anode SWS, then it helps in the formation of the electrons bunches, and the energy of the retarded electrons is transferred to the RF waves. MILO device consists of an interaction cavity which is in the number of more than three and it oscillates in its fundamental mode (i.e. in π -mode). The phase difference between these consecutive cavities of the interaction

structure is 180° and these cavities behave as a quarter-wave oscillator. In the π -mode, the maximum electric field exists at the tip of the disc and the maximum magnetic field at the top of the cavity which develops a spoke-like structure inside the device. The formed electron spoke is mainly responsible for beam-wave interaction in the device and finally, the electrons give up their potential and kinetic energy to the electromagnetic field. The generated RF signal is stored in the interaction structure in the form of a standing wave with a group velocity close to zero. To extract the stored energy out of the cavity, the extractor section is used.

RF Extraction: The RF energy is stored in the form of a standing wave inside the SWS cavities which is extracted out using an extractor cavity. The extractor mainly changes the standing wave into the traveling wave by slightly changing the group velocity of stored RF energy.

Thus the whole working mechanism of the MILO device can be explained in short as:

- High Voltage (400-600 kV) DC pulsed is applied between Anode- Cathode structure.
- Explosive electron emission starts at the cylindrical cathode surface.
- Intense electron emission causes a current density of $10^6 - 10^7$ A/cm² which creates ionized vapor state and plasma flares close to the cathode surface.
- Radial Electron motion creates a charging current which establishes magnetic insulation when it becomes equal to the critical current.
- Magnetic insulation helps in confining electron sheath between the tip of the disc and cathode along z-direction and creates Relativistic Brillouin flow (RBF).

- Due to the transient state, the electron sheath induces noise inside cavities and generates oscillation.
- Oscillation forms standing wave comprises of forward and backward TM_{00} space harmonics with identical frequencies, spaced symmetrically in π mode and amplified by beam-wave interaction.
- Stored EM energy inside the cavities coupled out through extractor coaxial section by a match of the extractor gap electric field with output coaxial transmission line.

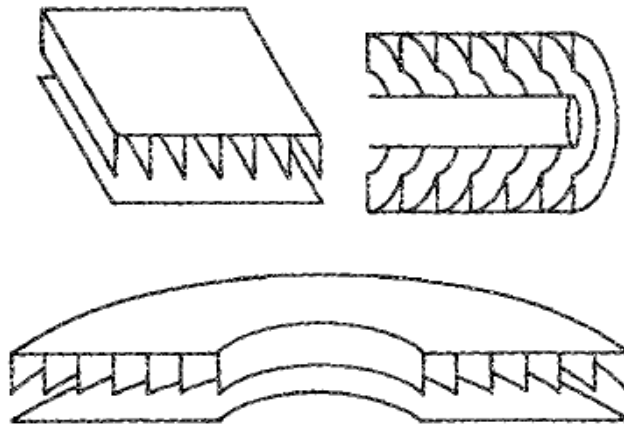


Figure 1.11: Different MILO configuration [Clark *et al.* (1988)].

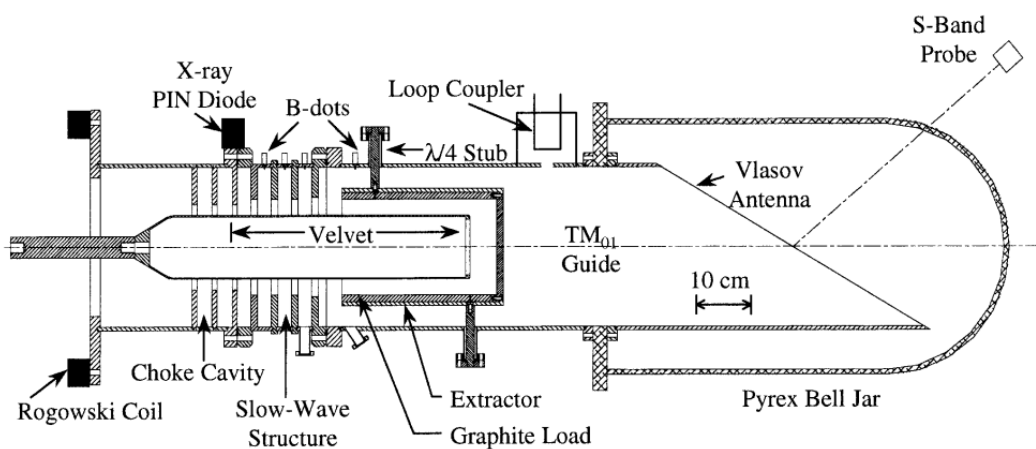


Figure 1.12: Configuration of Hard-tube MILO (HTMILO) [Haworth *et al.* (1998)].

1.4. Literature Review

The first breakthrough in the field of high-power microwave generation using a magnetically insulated line oscillator (MILO) was achieved by Clark *et al.* in 1988. They had used different geometries such as planar, coaxial, and concentric structures for MILO configuration which is given in Fig. 1.11. They had reported a simulation on MILO at 1.5 GHz frequency with efficiency 10% and performed an initial experiment with voltage 400 kV, current 50 kA, and pulse width 50 ns. It was concluded that MILO can be operated in line-limited and load-limited conditions for which load is placed at the end of the device, allowing independent adjustment of impedance.

In 1997, Lemke *et al.* investigated a non-linear regime in a load-limited MILO considering limitations on power conversion efficiency by using numerical simulation. They have given the theoretical aspect for load-length calculation, spokes formation, and efficiency estimation for the MILO device. The dc operating characteristics of MILO are determined by a current-carrying load which forms a part of a unique power extraction scheme. The maximum power is obtained when an RF choke is used for the upstream boundary and the maximum efficiency is accomplished by considering the spokes collectively as a modulated current crossing a voltage-modulated gap. The PIC Simulation of L-band MILO gave an output power of 3 GW for 493 kV, 56.2 kA with an efficiency of 10.8%. They have experimentally achieved peak power of 1.35 GW with an overall efficiency of 7.8% by applying an input voltage of 510 kV and a current of 34 kA. This work was carried forward by Haworth *et al.* with the motivation of significant pulse lengthening in 1998. The pulse shortening problem encounter by the MILO device because of spurious emission of electrons and asymmetry in MILO

design [Agee *et al.* (1996)]. Haworth *et al.* achieved an increase of the output power by 25% and an increase of the RF pulse duration by a factor of two and a half. They have used Hard-Tube MILO (HTMILO), build an all stainless steel, brazed version of the tube as given in Fig. 1.12.

In 1998, Eastwood *et al.* have presented a new MILO design with tapered SWS structure and axial power extraction. They have achieved 20% efficiency in *L*-band through simulation and further through experiment. The main feature of this design is its tapered SWS structure, its tapered multi extractor cavity, and diode gap. The diode gap mainly controls the load current and furthers the self-magnetic insulation inside the device. The use of tapered SWS structure helps in efficient beam-wave interaction, similarly, tapered extractor cavity gradually increases in the group velocity of RF generated and stored in SWS cavities which results in high efficiency of this device. The configuration used by Eastwood *et al.* is given in Fig. 1.13.

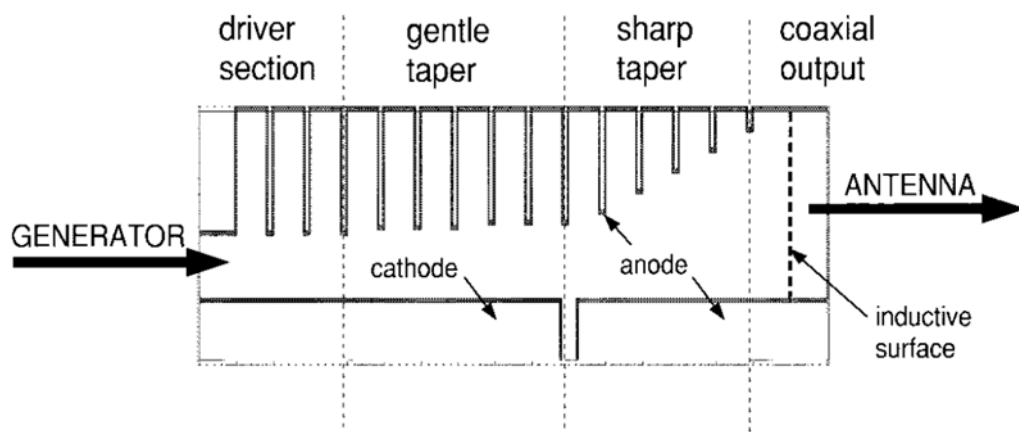


Figure 1.13: The configuration of tapered MILO [Eastwood *et al.* (1998)].

In 2007, Richard Cousin *et al.* reported a Gigawatt class of MILO that was driven by a low-impedance Marx generator. The operating frequency of 2.40 GHz is

confirmed by measuring the emitted radiation using both an in-vacuum antenna and a horn placed in the far-field region. The frequency response of the MILO was compared with 3D simulation performed with MAGIC. In the first experiment, microwave output peak power of 1 GW was obtained, which is in good agreement with the simulation results. Fan *et al.* in 2007, proposed a new kind of technique to reduce cathode length with a disc insertion inside collector or beam dump. In this design, the electron is emitted from both the curved surface as well as the end surface of the cathode. They have achieved through simulation and further validated through experiment, the peak power of 4.2 GW at a frequency of 1.76 GHz, with peak power conversion efficiency of 12%, when the voltage is 600 kV and the current is 52 kA. The configuration of the improved MILO design is given in Fig. 1.14.

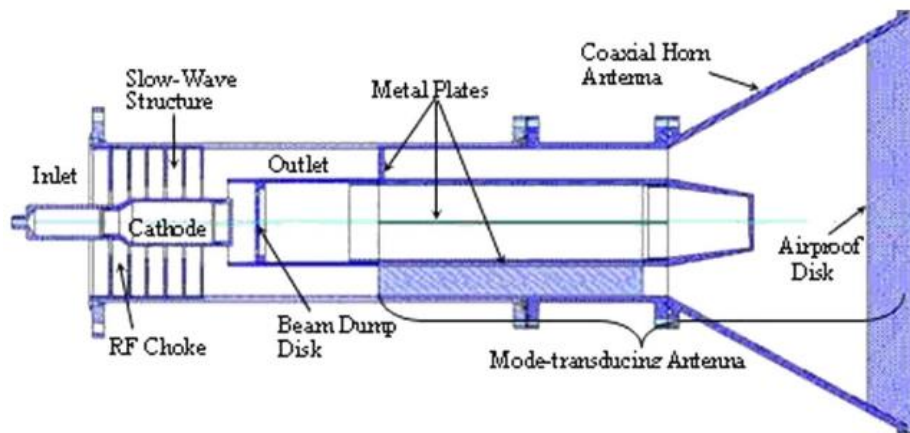


Figure 1.14: The configuration of the improved MILO [Fan *et al.* (2007)].

Fan Yu-Wei *et al.* in 2007 have proposed a double band high power microwave source for increasing the power conversion efficiency of MILO. The configuration of double band HPM source MILO is shown in Fig. 1.15. An axially extracted virtual cathode oscillator (VCO) was introduced to utilize the load current in the MILO. This is called the MILO-VCO configuration in which both are synchronized to generate HPM.

This was simulated of MILO-VCO using KARAT code and generated output power of 5.22 GW with an efficiency of 16.3%. In this MILO-VCO combination, the peak power of MILO is 3.91 GW at 1.76 GHz and the peak power of VCO is 1.33 GW at 3.79 GHz.

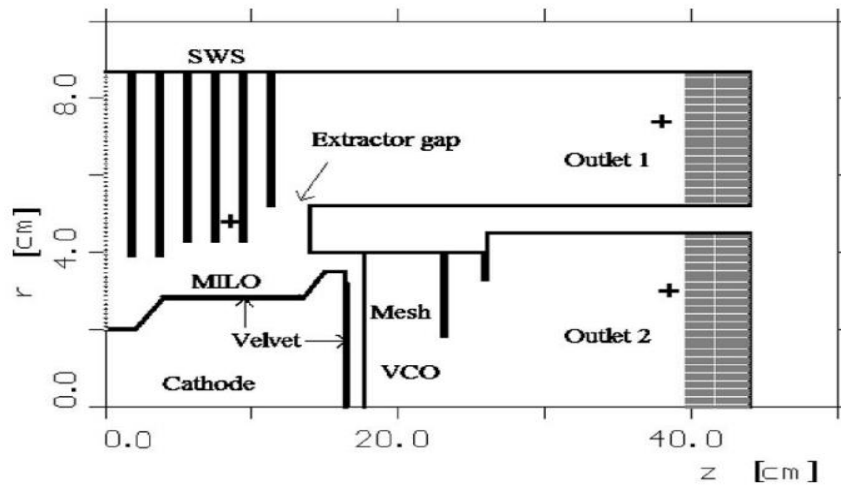


Figure 1.15: The configuration of MILO-VCO [Fan *et al.* (2007)].

Jin-Chuan Ju *et al.* in 2009, have investigated novel dual-frequency MILO with two separate, stable, and pure HPMs. The configuration of the design is given in Fig. 1.16. The dual-frequency MILO is divided into two MILO, MILO-1 in C-band and MILO-2 in the X-band. The simulated results showed that when the dual-frequency MILO is driven by an electron beam with 610 kV, 82 kA, the two HPMs are generated with a total power of 5.9 GW with power conversion efficiency is about 12%. MILO-1 generated power of 3.2 GW at 7.6 GHz and MILO-2 at 9.2 GHz with an output power of 2.7 GW. The proposed dual-frequency MILO has got two merits: (a) high efficiency (b) frequency adjustability.

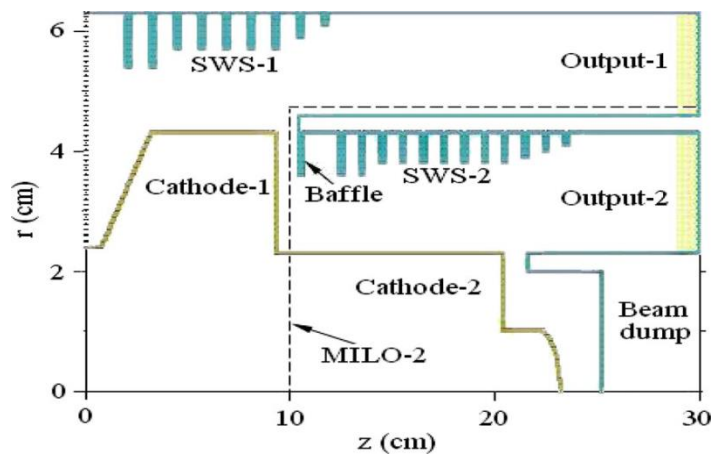


Figure 1.16: The schematic of the dual-frequency MILO [Ju *et al.* (2009)]

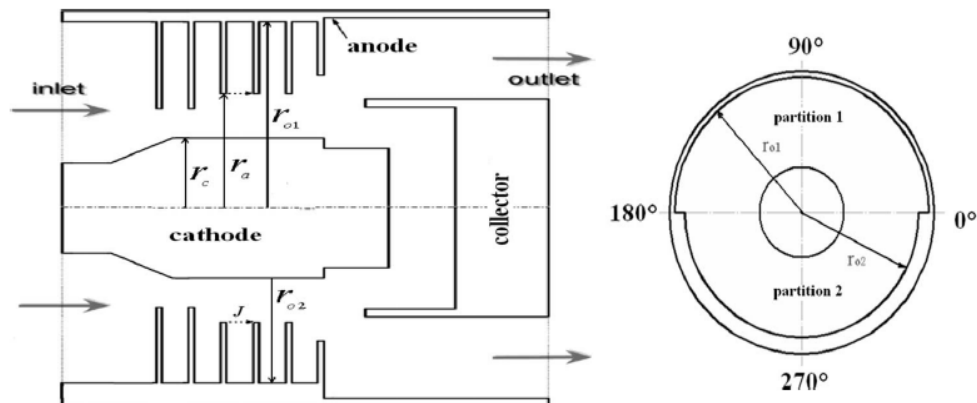


Figure 1.17: Bi-frequency MILO configuration: (a) axial view, and (b) front view.

In 2009, Dai-Bing Chen *et al.* have presented a bi-frequency (BF) MILO with a novel idea of azimuthal partition to generate HPM with the two frequencies of 3.4 GHz and 3.65 GHz in a single device. The configuration of bi-frequency MILO is given in Fig. 1.17. This MILO is realized by tuning the cavity-depth of a conventional MILO in an azimuthal direction along with the self-insulated current, total anode current, and total impedance as same as conventional MILO. The simulated C-band BFMILO stably yielded output power of ~ 1.43 GW for 490 kV, 45 kA with the power conversion

efficiency is ~6.5%. The amplitude difference between the two microwaves in the spectrum is about 0.4 dB.

A lot of theoretical work has also been done for the MILO device related to the analysis of its interaction structure in the absence and presence of an electron beam. Wang *et al.* in 2007 used a field matching technique to analyze the disc-loaded coaxial waveguide structure for both symmetric and asymmetric modes. In 2010, Wang *et al.* used field matching theory to analyze the periodic disc loaded coaxial structure with azimuthal partition. The equivalent circuit analysis for disc-loaded coaxial structure has been carried out for azimuthally symmetric TM_{0n} modes by Dixit *et al.* in 2016. Dwivedi and Jain in 2013, have optimized and enhanced the RF characteristics of the S-band MILO using MAGIC PIC code for 600 kV, 35 kA. This MILO device was analyzed for its designed value of 600 kV, 35 kA, and obtained 1.0 GW of RF output power with a power conversion efficiency of ~6% for the typical design parameters. The optimized S-band MILO structure produced the output power of 2 GW. Dixit *et al.* in 2017 have presented the design improvement for the efficiency enhancement of L-band MILO. They have achieved a maximum power conversion efficiency of 22.4 % through simulation. Nallasamy *et al.* in 2017 have presented electromagnetic simulation and experimental characterization of RF interaction structure of an S-band MILO. The cold test of RF interaction structure has been done using the 'CST studio suite' and further validated through experiment.

A literature survey related to the development of MILO design and its technological advancement for overall performance improvement is presented in table 1.3.

Table 1.3: Chronological order of development of MILO device.

Year	Title	Author/Lab	Frequency	Input Voltage/ Current	O/P power/ Rep. rate	Efficiency
1997	Load-Limited MILO	R. W. Lemke <i>et al.</i> / USAF Lab	1.18 GHz	510 kV, 34 kA	1.35 GW, Single shot	7.7%
1998	Pulse lengthening multi GW MILO	M. D. Haworth <i>et al.</i> / USAF Lab	1.2 GHz	500 kV, 60 kA	1.875 GW,	6.6%
1998	The Tapered MILO	J. W. Eastwood <i>et al.</i>	1 GHz	440 kV, 30 kA	1.35 GW	10.5%
2007	Compact MILO	R. Cousin <i>et al.</i> / LPTP France	2.4 GHz	500 kV, 45 kA	1.35 GW	6%
2007	Improved MILO	Y. W. Fan <i>et al.</i>	1.74 GHz	550 kV, 57 kA	2.4 GW	7.6%
2008	Giga watt MILO	D. H. Kim <i>et al.</i>	1 GHz	466 kV, 34 kA	1.82 GW	11.5%
2008	Improved MILO with the high rep. rate	Y. W. Fan <i>et al.</i>	1.755 GHz	510 kV, 54 kA	2.17 GW, 20 Hz rep. rate	7.9%
2008	X-band MILO	Y. W. Fan <i>et al.</i>	9.7 GHz	400 kV, 50 kA	110 MW, Single shot	>1%
2009	S-band Tapered MILO	M. D. Li Zhi-Qiang <i>et al.</i>	2.63 GHz	500 kV, 35 kA	2 GW,	11%

2009	Bi-Frequency MILO	Dai-Bing Chen <i>et al.</i>	1.26 GHz & 1.45 GHz	420 kV, 34 kA	620 MW	4.2%
2013	Ku-Band MILO	Jie-Wen <i>et al.</i>	12.9 GHz	539 kV, 57 kA	89 MW	>1%
2015	Metal Dielectric cathode MILO	Xiaoping Zhang <i>et al.</i>	1.562 GHz	425 kV, 34 kA	1.95 GW	13.5%
2015	Improved Ku- band MILO	Tao-Jiang <i>et al.</i>	13.02 GHz	450 kV, 45 kA,	150 MW	>1%
2015	Complex dual-band HPM source	Xiaoping Zhan <i>et al.</i>	MILO-2.1 GHz and VCO-3.8 GHz	440 kV, 35 kA	MILO -1.7 GW VCO-0.37 GW	13.4%
2016	High efficient rep. pulsed MILO	Yu-Wei Fan <i>et al.</i>	1.598 GHz	420 kV, 40 kA	2.1 GW, With 5 Hz	15.5%
2016	MILO with metal array cathode	Fen Qin <i>et al.</i>	1.56 GHz	544 kV, 60 kA	2 GW	6.3%
2016	Tunable MILO	Yu-Wei Fan <i>et al.</i>	1.337-1.760 GHz	430 kV, 40.6 kA	1.51 GW-2.653 GW	8.7-15.2%
2017	Carbon fiber array cathode HTMILO	An-Kun Li, Yu-Wei Fan, and Bao-Liang Qian	1.56 GHz	460 kV, 48 kA	2.9 GW	13.1%
2017	Vacuum-sealed repetitively pulsed MILO	Tao-Xun <i>et al.</i>	1.58 GHz	630 kV, 48 kA, Rep-rate: 5 Hz	3.4 GW	11.24%

2017	Ku-band MILO with Tapered choke cavity	Tao- Jiang <i>et al.</i>	12.36 GHz	515 kV, 48 kA	1.2 GW	4.85%
2019	Ridged Disk-Loaded MILO	Xiaoyu Wang <i>et al.</i>	1.48 GHz	566 kV, 50 kA	6 GW	21% (Simulation)
2020	Novel High-Efficiency MILO	Xiaoyu Wang <i>et al.</i>	1.42 GHz	586 kV, 49 kA	6.3 GW	22% (Simulation)

1.5. Motivation and Research Objective

The motivation for the present research on HPM source MILO is led from its potential application particularly in defence. In the last few years, MILO emerged as one of the most promising HPM source due its compactness, lightweight, and efficiency which enables it to use as a direct energy weapon and can also be mounted on the mobile platforms. Significant works for overall performance improvement of MILO device has been carried out in the past and present days which include theoretical, experimental, and simulation work. The dual-frequency generation through a single HPM device by using different design methodology and concept is one of the interesting research areas these days. The designing improvement of MILO to avoid some critical issues like pulse shortening problem, asymmetric mode generation and mode competition, shot-to-shot reproducibility, requirement of high pulse rate frequency and long life of cathode are still consider as a challenge for device development. MILO is a high-power pulsed microwave source which uses a high DC pulse for its operation. This high DC pulse have some rise time, hold time and fall time. But during its experiments which are reported in the literature, the device suffers from pulse shortening problem. When this

device is operate for pulse repetition (i.e. more than two similar DC pulses) then the RF pulse generated at the output do not show similar behavior for each and every input DC pulses. This problem is termed as “shot to shot reproducibility”. This problem generally occurs when large number of stubs are used at the output side of MILO. These aspects motivated the author to associate, contribute, and enhance the knowledge for the HPM oscillator — MILO device.

The prime objective of the thesis is to contribute research work for performance improvement of MILO and bi-frequency MILO. In order to carry out the aforementioned work, the author considered the optimization of the MILO device sub-assemblies and impedance matching between different sub-assemblies using the equivalent circuit approach. Further, the study of beam-wave interaction for the generation of bi-frequency through MILO device is also taken as the objective for current work. The analysis for the same in the absence and presence of the electron beam are carried out adapting the equivalent circuit approach.

1.6. Plan and Scope

As per the application point of view, the MILO device is found as one of the most accepted HPM devices because of its self-magnetic insulation, compactness, and lightweight characteristics. This device does not change the operating frequency by just changing the input DC voltage which makes it stable for a large voltage range. For the generation of bi-frequency through a single HPM device, MILO has more potential among the HPM devices. In the field of HPM source, MILO designing and experimental work is always a challenging task due to the involvement of various fields electromagnetic theory; charge particle; optics; dissipation of sufficient amount of

power at the anode; plasma formation; thermal effects at the load side, etc. Therefore, to explore these aspects, it has been planned to further improve the analysis, design, simulation, and the experimental activities for MILO. The impedance matching between different sub-assemblies of MILO is required for its performance improvement which is planned to be carried out adapting the equivalent circuit approach. The bi-frequency generation is also planned to be studied using the analytical approach and validation of the analysis through PIC simulations. Thus, the whole research work considering the above-mentioned objectives is embodied in the form of the present thesis which is organized in the seven chapters as follows:

In chapter 1, the overview of different HPM systems, their applications, and needs in different domains are described. An overview and comparison of different HPM sources are described briefly and found that the MILO device is an attractive HPM source for generating high power microwaves among them. A brief description of different sub-assemblies of the MILO device and the principle of operation are presented in this chapter. A detailed literature review of the development of theory, design, and development of the MILO device is presented. Finally, the motivation and objective of the current thesis work are also explained here.

Chapter 2, the equivalent circuit analysis used to understand the MILO beam-wave interaction is reviewed. The different analytical approach developed for analysis of the RF interaction structure used in MILO and other HPM sources is briefly reviewed with their limitations comparison. The EM field expressions and boundary conditions for analysis of MILO device in the absence and presence of the electron beam are presented which helps in obtaining the expressions for the equivalent circuit line parameters. The equivalent circuit line parameters are required for finding MILO device

design characteristics, like, dispersion relation, phase velocity, group velocity, and characteristic impedance.

In Chapter 3, the designing issues of the different subsection of the device are studied with the aim to improve the performance of the MILO. Presently MILO device analytical, simulation, and experimental studies have been reported extensively; however, device performance optimization studies are limited to experimental and simulation studies. In this present work, analytical studies of the device performance improvement and optimization have been carried out, a study useful for device developers. Here, in this chapter, for the first time the impedance matching approach have adapted for this purpose. Impedances of the different MILO subassemblies are matched to minimize the reflection and maximize the RF power transfer inside the device. For this purpose, an equivalent circuit approach has been used. First, the input impedance of the tapered inner conductor of the coaxial structure is matched with the impedance of the choke discs. Then the extractor inner radius and extractor gap impedance are optimized at the output section of the device. This impedance matching scheme helps in achieving the maximum efficiency from the device with optimum RF transmission. Finally, to validate the presented concept, initially an experimentally reported L-band MILO is simulated using commercial (particle-in-cell) PIC code and planned to be validated with the experimental values available in the literature. Further, the PIC simulation with the optimized design parameters is to be performed which will provide further improvement in the MILO device RF output power.

In chapter 4, an equivalent circuit approach is used to investigate the bi-frequency generation by the azimuthally partitioned axially periodic metal disc loaded coaxial structure. This analysis has been done for the first time which eliminates the limitation

of previously developed equivalent circuit approach and provides a tool to completely analyze coaxial disc loaded structure which has potential to generate bi-frequency. The EM field distributions generated inside this structure exhibits both axial and azimuthal harmonics therefore the individual TE or TM mode no longer satisfies the boundary conditions. Thereby the EM eigenmodes within the device are having all the six components of electric and magnetic fields resulting in hybrid modes (HEM modes) generation inside the structure. Thus, the present approach can be used for all kind of coaxial structure which is either be azimuthally symmetric or azimuthally partitioned. Considering the effect of all harmonics present within the structure and using an equivalent circuit approach, the expression of the equivalent series inductance per unit length and equivalent shunt capacitance per unit length are obtained for this equivalent transmission line. In addition, with the help of computed equivalent series inductance and equivalent shunt capacitance, expressions for the dispersion relation, phase velocity, and characteristic impedance are also to be obtained. Further, the maximum possible frequency difference (i.e. bandwidth) between the modes (i.e. resonating frequency) and their region of operation, are analytically computed. Finally, parametric studies are performed to find out the effect of structural parameter variation on dispersion behavior. In order to validate the numerical analysis, the structure is firstly simulated with the help of a commercial code “CST Studio Suite” and then the analytically obtained results (such as dispersion behavior and phase velocity) are compared with the results obtained from the simulation.

In chapter 5, the electromagnetic behavior of the azimuthally partitioned axially periodic metal disc loaded coaxial structure in the presence of the electron beam using an equivalent circuit approach is presented. This work is the novel work done for the

first time which provides the complete analytical tool to insight of the beam-wave interaction process for generation of bi-frequency using interaction structure formed by azimuthally partitioned axially periodic metal disc-loaded coaxial structure. Also, this helps in estimating the RF power generation and energy stored inside the interaction cavities through analysis. Since the EM eigenmodes within the device having all the six components of EM fields, thereby in this analysis we have considers both type modes (i.e., symmetric and asymmetric mode) for beam-wave interaction. In the analysis, the linearized maxwell's fluid equation (also known as Vlasov-Maxwell's equation) has been used in the electron beam-present region. The expression for the dispersion relation and temporal growth rate is obtained using equivalent line parameters.

In chapter 6, the device design and PIC simulation of the bi-frequency MILOs are presented. The expressions of design parameters and the procedure to design the bi-frequency MILO are described in this chapter. Further, the PIC simulation of L-band and S-band bi-frequency MILO and S/Ku dual-band MILO are presented in detail.

Finally, in chapter 7, the work described in this present thesis is summarized and significant conclusions are drawn from the major findings. The limitations of the the present study is also discussed pointing out the scope for further work.